# Nickel Carbonate Precipitation in a Fluidized-Bed Reactor

**ARTICLE** *in* INDUSTRIAL & ENGINEERING CHEMISTRY RESEARCH · OCTOBER 2001

Impact Factor: 2.59 · DOI: 10.1021/ie010312q



**2 AUTHORS**, INCLUDING:

Alison Lewis
University of Cape Town
**61** PUBLICATIONS **684** CITATIONS

MATERIALS AND INTERFACES

# Nickel Carbonate Precipitation in a Fluidized-Bed Reactor

**Damien Guillard and Alison E. Lewis***

*Precipitation and Crystallization Research Facility, Chemical Engineering Department, University of Cape Town, Rondebosch 7701, South Africa*

Carbonate precipitation of nickel in pellet reactors has several advantages over the more commonly used hydroxide sludge process. As a seeded precipitation, no sludge is formed; instead, there is a dense precipitate permitting easy solid−liquid separation and reuse of the nickel by dissolving the pellets. Furthermore, carbonate precipitation occurs at a lower pH, thus reducing the postneutralization costs of the stream. A laboratory-scale fluidized bed was used in order to study the precipitation processes relevant for pellet reactor technology. Different profiles of the bed were established to determine the relative importance of the various precipitation phenomena such as homogeneous and heterogeneous nucleation. The rapid kinetics of nickel carbonate nucleation, driven by high local supersaturation, formed a large amount of fines that agglomerated slowly up the bed. In general, the nickel removal efficiency not only was solubility dependent but was largely influenced by the fines nucleation, and thus by the supersaturation profile of the reactor.

## Introduction

As environmental release standards and economic constraints become tighter, industry is placing a greater emphasis on the treatment of metal-containing effluents. Several techniques have been developed to recover metals, such as evaporation, ion exchange, and electrolysis. The most commonly used process is precipitation,[1] because it offers a cost-effective solution applicable to large operating units. For heavy metals such as zinc, copper, manganese, lead, and nickel, hydroxide precipitation is generally used for large-scale plants, although it has many drawbacks. The metal is recovered as a sludge without any commercial or industrial value. It also has poor dewatering characteristics[2] and produces voluminous sludges that must be stored in waste landfills.[3] Also, the optimum precipitation occurs at relatively high pH, around 10.5−11,[4] which increases the cost of postneutralization of the streams.

Considerable effort is being expended to develop more efficient precipitation processes. The development of heavy-metal precipitation in pellet reactors is one proposed method to improve metal recovery at lower cost. Pellet reactor technology has been developed for softening of drinking water[5] as well as for removal of phosphates from wastewater.[6] Since the early 1980s, this technique has been extended to the removal of heavy metals,[7,8] using carbonate as a precipitating agent. In the literature,[7,8] treated concentrations range from 10 to 100 000 ppm of metal from various waste streams such as acid mine drainage, electroplating, and base metal refining.

The pellet reactor provides an ideal environment for controlled crystallization in a stable and easily operated process. The large crystal surface area provided by the pellets favors heterogeneous nucleation on the seeds and allows operation with a slightly supersaturated solution that avoids spontaneous nucleation of fines that are not easily separated from the stream. The relatively high fluid velocity in the reactor, typically in the range of 10−35 cm/s,[9] prevents the cementing of the pellets by providing their fluidization. Good mixing of the reactants also occurs.

Using this technology, a dense precipitate of metal carbonate is obtained directly onto the pellets. Sludge formation and related problems are avoided, and the metal salt covering the seeds can then be recovered in concentrated solution by dissolving the deposit on the pellets in a strong acid. The carbonate escapes as carbon dioxide, and the metal is recovered in a concentrated form that can easily be reused in industry. The seeding material can also be reused in the reactor. The system has both economic and environmental advantages.

This paper focuses on the precipitation of nickel carbonate from a synthetic nickel sulfate stream, using a laboratory-scale pellet reactor. The main contribution of this work is an examination and explanation of the various precipitation mechanisms occurring in the reactor through the measurement of various profiles up the length of the bed.

## Nickel Precipitation: Nickel Hydroxy−Carbonate Solubility Diagram

Solubility diagrams are used in order to predict the precipitation efficiency, but in many cases, the determination of all of the species present in solution is impossible, and it is essential to define the concept of a general “solubility domain” that encompasses the main species of interest. The solubility domain is constructed

10.1021/ie010312q CCC: $20.00 
Published on Web 10/23/2001

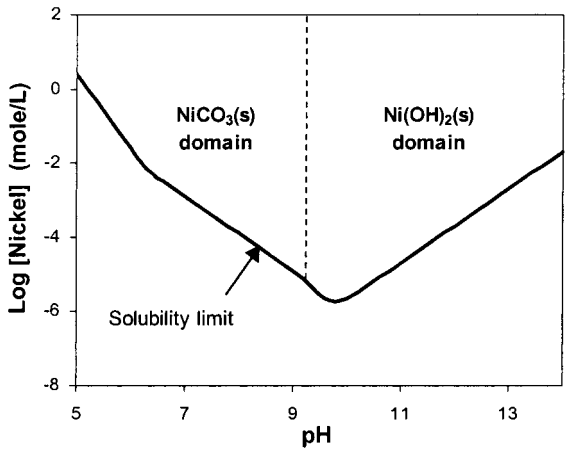


**Figure 1.** Nickel hydroxide−carbonate.

through interpretation of the thermodynamic and kinetic constants from the literature. The solubility domain of nickel in this case has to be defined for a solution containing numerous ions, because nickel carbonate precipitation never occurs alone but in competition with nickel hydroxide precipitation. The final solubility domain will be determined from a superposition of the hydroxide and carbonate solubility diagrams as developed by Patterson et al.[2] See also Stumm and Morgan[10] for a general description of equilibrium models. The mononuclear hydroxy complex species considered here are $Ni(OH)^+$ and $Ni(OH)_3^-$, with the composition of the solid-phase being $Ni(OH)_2(s)$.[11] Complexes of Ni with carbonate [$NiCO_3(aq)$, $NiHCO_3^+$, and $Ni(CO_3)_2^{2-}$] were disregarded.

The equilibrium reactions used in the construction of the solubility diagram can be found in work by Patterson et al.[2] For this relatively dilute system, it was assumed that activities could be replaced by concentrations.

The Ni−OH−$CO_3$ solubility diagram is drawn as a function of pH and $C_T$ ($C_T = 10^{-3}$mol/L of carbonate species). The predominating solubility domain for each compound of the solid phase is delimited on the solubility diagram (Figure 1). Below pH = 9.2, nickel carbonate salt is the predominating solid phase, whereas at higher pH, the dominant solid phase is that of nickel hydroxide. In practice, no real boundary can be observed, and the solid phase is more likely to be a mixed complex of nickel hydroxy−carbonates, whose composition is expected to depend on the carbonate-to-nickel ratio within the reactor, e.g., $Ni(CO_3)_{0.22}(OH)_{1.56}$ or $Ni(CO_3)_{0.34}(OH)_{1.32}$.[7] From the diagram, the pH for the lowest solubility is found to be approximately 9.8.

## Experimental Methods

**Reactor Design.** The pellet reactor consisted of a cylindrical vessel of 1 m height and 0.025 m i.d. sealed from the atmosphere (Figure 2). The major control parameters of the reactor are the feed rate, the recirculation rate, the operating pH, the height of seeds at zero flow, and the multiple feed (not used during this phase of the experimental work).

The bottom of the column consisted of a conical glass fitting incorporating a plastic nozzle with large holes. This fitting was filled with glass beads of decreasing diameters that allowed uniform distribution of the upward flow as well as provided a support for the seeds (Figure 3). The reactor was filled with a narrow particle

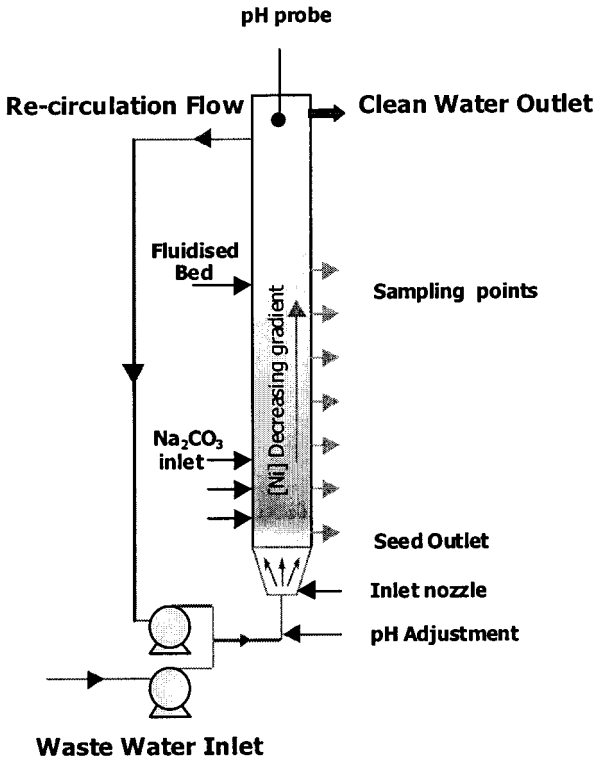


**Figure 2.** Schematic representation of the pellet reactor.

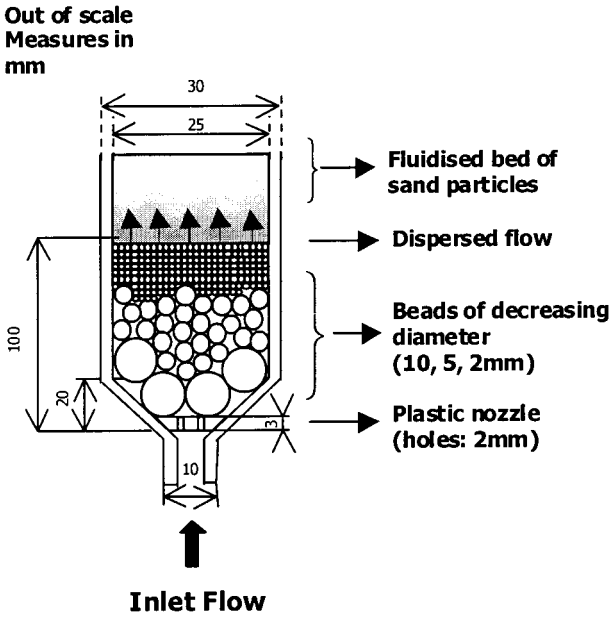


**Figure 3.** Pellet reactor inlet nozzle.

size distribution (50−70 mesh), white quartz sand mixed with calcite and aragonite [X-ray diffraction (XRD) analysis]. The height of the bed at rest was 60 ± 5 cm, and fluidization was achieved mainly through the recirculation flow (a maximum recirculation ratio of 1.66 to the inlet stream).

There were up to three possible inlets for the carbonate solution on the side of the column. Each inlet was controlled with a separate valve and consisted of a steel tube of 1 mm i.d. The inlets were spaced every 10 cm, starting 15 cm from the bottom of the bed. For this phase of the experimental work, only one bottom inlet was used.

There were seven sampling points (10 mm o.d.), spaced every 10 cm from the bottom of the column

(Figure 2). The outlet points allowed the withdrawal of solution as well as pellets from the reactor at different heights. At the top of the column, there were two similar outlets (a glass tube of 10 mm o.d.) that were used for the recirculation flow and the reactor outlet. The recirculation flow was used to increase the residence time of the nickel in the reactor, as well as to provide a dilution of the inlet stream at the bottom of the reactor.

**pH Control.** A pH probe was situated at the top of the column, allowing continuous monitoring of the system pH. The operating pH varied between 8 and 11 and was maintained by addition of acid or base in the recirculation loop. The pH pump was a custom-made pump that allowed very small flow rates, and the pH adjustment solutions were 0.01−0.1 M hydrochloric acid and sodium hydroxide, respectively. Under normal operating conditions, the operating pH was very stable because of the buffering effect of the carbonates and the recirculation flow.

**Reagents.** Precipitation was achieved by mixing a pure nickel sulfate solution with sodium carbonate. The synthetic nickel solution fed to the reactor had a concentration of 50−150 ppm of nickel ($8.5 \times 10^{-4}$−$2.6 \times 10^{-3}$ mol/L) depending on the experiment, a reflection of the typical effluent stream concentrations encountered in industrial situations. This corresponds to a nickel load of 367−1098 g/h/m$^2$ reactor cross-sectional area. The solution was prepared with nickel sulfate hexahydrate (MM = 262.8 g/mol) dissolved with tap water containing less than 0.1 ppm ($1.7 \times 10^{-6}$ mol/L) of nickel and $8 \times 10^{-4}$ mol/L of carbonates. The carbonate solution had a concentration of $2.8 \times 10^{-3}$−$3.4 \times 10^{-2}$ mol/L of carbonate. This corresponds to a relative carbonate-to-nickel ratio of 1:1 to 4:1 when fed to the reactor. The carbonate used was anhydrous sodium carbonate (MM = 105.99 g/mol). The flow rates of nickel and carbonate solutions were constant ($Q_{Ni}$ = 3.6 L/h and $Q_{CO_3}$ = 1.08 L/h), and the temperature of the bed and solution was 24 ± 3 °C.

**Particle Size Profile.** The coating of the pellets by the precipitate is responsible for a change in the particle size distribution of the pellets as well as a change of their density. Related to this phenomenon, the great mobility of the particles through the fluidized bed is responsible for the establishment of a gradient of the particle size within the height of the bed. The heaviest particles, which are less entrained by the fluid, settle at the bottom of the bed, while the lightest float over the bed. The biggest particles can then be easily removed from the bottom of the reactor, and new seeding material is introduced at the top, while operating in a continuous process. The seed addition and pellet removal were carried out intermittently.

**Sampling/Analysis.** Samples were taken from the side of the bed and from the top outlet. These were used to determine the nickel removal efficiency as well as to establish concentration and pH profiles of the fluidized bed. For every sample drawn from the column, half was filtered using a 0.45 $\mu$m filter, with the other half being left as drawn. A comparison of the total and dissolved nickel was then possible. The two half samples were then acidified with 5 drops of 0.1 M hydrochloric acid to prevent further precipitation and to allow the redissolution or digestion of the fines.

The nickel sample analysis was carried out using atomic adsorption spectrophotometry. The carbonate concentrations were determined by two different titration techniques: a colorimetric titration with a 0.1 N hydrochloric acid standard solution combined with a mixed indicator (methyl orange−indigo carmine); a pH-metric method using the same titration standard. The analyses of the pellets were carried out using XRD, X-ray fluorescence (XRF), and scanning electron microscopy (SEM) techniques.

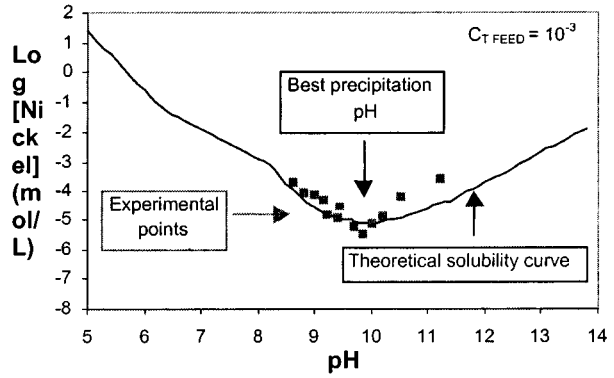


**Figure 4.** Solubility results: $C_{T\,FEED} = 10^{-3}$ and $CO_3$/Ni mole ratio = 2.

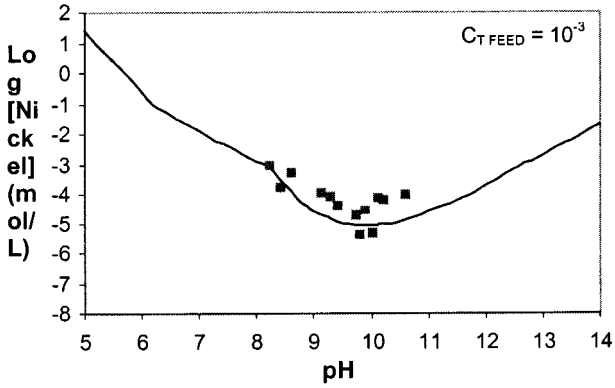


**Figure 5.** Solubility results: $C_{T\,FEED} = 10^{-3}$ and $CO_3$/Ni mole ratio = 4.

## Results and Discussion

**Comparison of Theoretical versus Observed Solubility.** Figures 4 and 5 show a comparison of theoretical and actual nickel carbonate solubilities for one set of operating conditions. These data were collected for $CO_3$/Ni ratios of 2 (Figure 4) and 4 (Figure 5). In general, the variability in the measured results is relatively high, with the standard deviation being 0.2 ppm ($3.4 \times 10^{-6}$ mol/L) for dissolved nickel and 2.4 ppm ($4.1 \times 10^{-5}$ mol/L) for the total nickel (including fines). It can be seen that for a ratio of 2 there is relatively good agreement between the experimental points and the theoretical solubility curve from pH ≈ 8 until pH ≈ 10.5. Above pH = 10.5, the experimental points lie significantly above the theoretical solubility curve. For the experimental points collected for a ratio of 4, a discrepancy with the theory is observed over a much larger pH range, starting at pH = 8.5. The optimal removal is obtained at a pH of 9.8 irrespective of the carbonate-to-nickel ratio. In fact, the theoretical model can predict the nickel conversion but cannot be used for the prediction of removal because of the presence of fines. See the Discussion section.

**Optimal Precipitating pH.** Figures 6 and 7 show the effect of pH on the nickel removal efficiency (eq 1), nickel conversion (eq 2), and fines formation during two

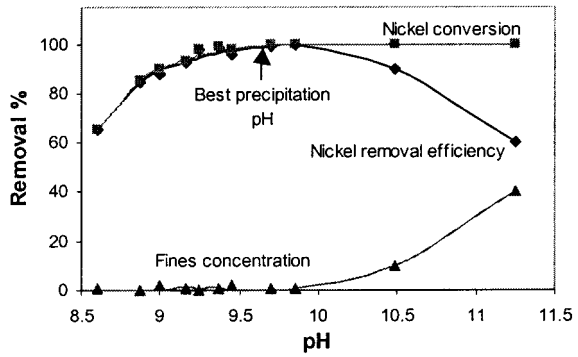


**Figure 6.** Effect of pH on the nickel removal efficiency, nickel conversion, and fines formation: $C_{T\,FEED} = 10^{-3}$ and $CO_3$/Ni ratio = 2.

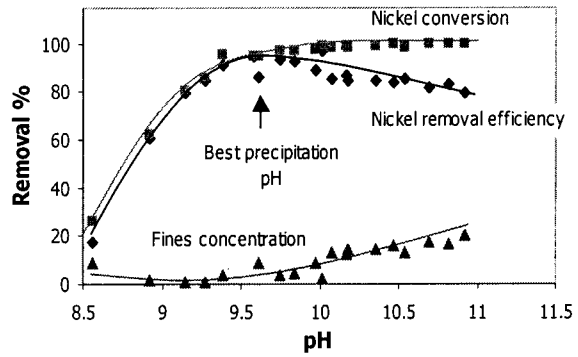


**Figure 7.** Effect of pH on the nickel removal efficiency, nickel conversion, and fines formation: $C_{T\,FEED} = 10^{-3}$ and $CO_3$/Ni ratio = 4.

sets of experiments at carbonate-to-nickel ratios of 2 (Figure 6) and 4 (Figure 7). The fines concentration is plotted on the figures as a percentage of introduced nickel.

nickel removal efficiency:

$$\eta\,(\%) = \frac{\mathrm{Ni_{in}} - \mathrm{Ni_{out,total}}}{\mathrm{Ni_{in}}} \times 100 \quad (1)$$

where $\mathrm{Ni_{in}}$ = nickel concentration in the feed (mol/L) and $\mathrm{Ni_{out,total}}$ = nickel concentration in the outlet (including fines) (mol/L).

nickel conversion:

$$\chi\,(\%) = \frac{\mathrm{Ni_{in}} - \mathrm{Ni_{out,dissolved}}}{\mathrm{Ni_{in}}} \times 100 \quad (2)$$

where $\mathrm{Ni_{in}}$ = nickel concentration in the feed (mol/L) and $\mathrm{Ni_{out,dissolved}}$ = dissolved nickel concentration in the outlet (mol/L).

From the figures, it is apparent that the nickel conversion increases steadily with increasing pH until pH $\approx$ 9.8 and then levels out at a value of near 100% for both ratios. The curve for the nickel removal reaches a maximum at pH $\approx$ 9.8 for both experiments. First, the removal increases with increasing pH and thus increasing nickel conversion and reaches peaks of 99.6% (ratio 2) and 97.2% (ratio 4) at pH $\approx$ 9.8. Thereafter, the efficiency decreases again with increasing pH, and the fines appear in the outlet. The formation of fines is minimal until pH $\approx$ 9.8, whereafter it begins to increase, reaching maximum values of 40% (ratio 2) and 20% (ratio 4) coinciding with the maximum measured pH value. In contrast to ratio 2, fines remain in the outlet over the whole pH range of the ratio 4 experiment.

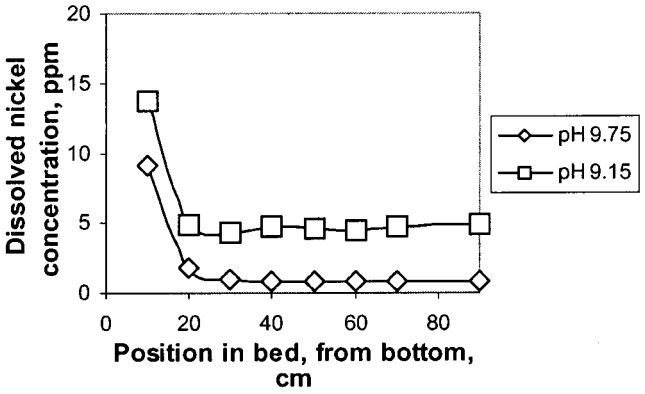


**Figure 8.** [Ni] dissolved profile within the fluidized bed.

**Bed Profiles. (a) Dissolved Nickel Profile (Figure 8).** Each line was measured during a different experiment, working at fixed outlet pH's of 9.15 and 9.75, respectively. In each case, the decrease in the dissolved nickel concentration occurs within the first 20 cm of the bed, after which the concentration reaches a relatively steady level as the soluble nickel reaches its solubility limit: 4.6 ppm ($7.8 \times 10^{-5}$mol/L) at pH = 9.15 and 0.85 ppm ($1.4 \times 10^{-5}$mol/L) at pH = 9.75. The steep slope of the dissolved nickel concentration curve when decreasing shows the fast kinetics of the precipitation reaction. For this case, the two slopes are very similar. Their average is a loss of 0.81 ppm ($1.38 \times 10^{-5}$mol/L)/cm of bed. The state of near equilibrium with the solid phase is reached a few seconds after the mixing of the reactants, and no further significant conversion is measured upward in the bed.

**(b) pH Profile (Figure 9).** Each of the lines represents a different pH set point, which is monitored and controlled through the pH probe at the top of the column. The set points were pH = 9.75, 9.4, 9.2, 9.15, and 8.4. For all but one of the set points, the pH values are the lowest at the bottom of the bed. For the set points of 9.75, 9.4, 9.2, and 8.4, the pH profiles experience a peak at the carbonate injection point, because the incoming carbonate solution causes the pH to increase. Thereafter, the pH steadily decreases an average of 0.2 pH units through the bed height, because of slow supersaturation consumption over the remainder of the bed. For the set point of 9.15, the increase in pH over the height of the bed is much more gradual, with the highest pH value occurring at sample point 4.

**(c) Pellet Analysis.** XRD, XRF, and SEM techniques were carried out on the pellets drawn from the bottom of the bed. The precipitate on the pellets was identified as a 2 $\mu$m deep amorphous layer after 24 h of experiments. Elemental analysis showed the presence of traces of calcium, potassium, and manganese in the precipitate (coming from the tap water), but more than 98.2% of the metal present was nickel. The exact composition of the precipitate, and especially the ratio of nickel to carbonate to hydroxide, was not established precisely and will be the subject of a later study. The surface of the pellets was smooth, probably the result of friction and attrition between the pellets. The layer of precipitate cracked when dried.

## Discussion

The solubility model previously discussed must be used with caution when predicting the conversion in the

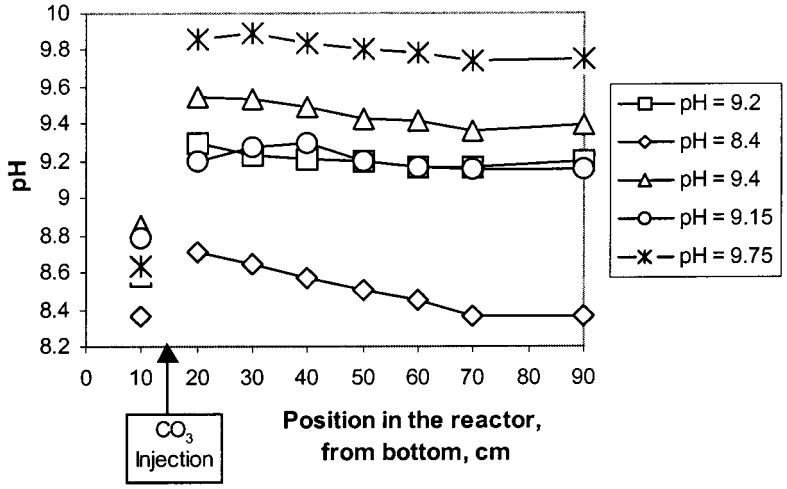


**Figure 9.** pH profile within the fluidized bed.

reactor for two reasons. Deviations from the theoretical solubility can first be observed because of a lack of information concerning the equilibrium between the phases. The presence of discrepancies between the solubility constants found in the literature, the presence of other insoluble metal hydroxides and carbonates, the lack of equilibrium conditions, ionic strength effects, analytical inability to precisely separate the colloidal precipitate, and the presence of impurities and complexing agents[12,13] are the main sources of discrepancies. Discrepancies in solubility constants would negate the assumption based on specific solubility constants made in constructing the solubility diagram, and the presence of other species and complexes would negate the simplifying assumption that only certain aqueous and solid species are present.

The second reason is due to the nature of the pellet reactor itself, because the nickel in the outlet stream can occur both as dissolved nickel and as fines. Consequently, the solubility of the product is not the only parameter playing a role in the nickel removal. Some fines are also washed out with the outlet stream, and these are not classified as being part of the nickel removal. Fines can be formed either by attrition of the precipitate already on the pellets or by primary nucleation occurring in the bulk of the solution, as illustrated in Zhou et al.[8] Given sufficient residence time in the reactor, the fines can agglomerate onto the pellet. This mechanism is supported by the measured pH and dissolved nickel profiles up the length of the bed in Figures 8 and 9. The profiles suggest a first rapid precipitation reaction followed by slow supersaturation consumption by agglomeration of primary particles upon the grains. The undetected change in nickel concentration in the pH range 9−10.5 is compatible with the pH change of approximately 0.2 units, as evidenced by the flatter part of the solubility curve in Figure 4. A similar behavior of a pellet reactor has been reported for phosphate precipitation.[6]

The precipitation mechanisms are closely linked to the local supersaturation at different points within the bed. Local supersaturation is high at the reactant inlet and decreases further up the column, away from the inlet. Low supersaturation favors the crystal growth of the precipitate and the heterogeneous nucleation on the seeds, i.e., the enlargement of the size of the pellets, whereas a high supersaturation leads to the formation of new crystal matter within the liquid medium, or fines, by spontaneous primary nucleation.[14,15] The supersaturation is dependent on both carbonate and hydroxide concentrations, because they represent the competitive precipitating systems. Regions of high local supersaturation develop at the reactant inlets at high $CO_3^{2-}$ concentrations and in the whole reactor at high pH, and this leads to the spontaneous nucleation of a solid phase within the liquid medium. This phenomenon explains the presence of the discrepancies between solubility and removal observed in Figures 4 and 5 and explains why a higher carbonate-to-nickel ratio does not cause an improvement in the nickel removal. Thus, at pH = 9.8, the removal of the nickel reaches 99.6% for a ratio of 2 (Figure 6) and only 97.2% for a ratio of 4 (Figure 7), while the nickel conversion exceeds 99.8% in both experiments. The generation of a significant amount of fines due to high concentrations of hydroxides is illustrated by the two deviating data points found at high pH values (above pH = 10.5) in Figure 6 (ratio 2).

The general efficiency of the process could be improved by the addition of a postfiltration stage. With filtration, the process can remove more than 99.9% of the initial nickel under optimum conditions, and less than 0.1 ppm ($1.7 \times 10^{-6}$ mol/L) is found in the treated stream when filtered. This is evidenced by the filtered samples taken and used to obtain the data points for "nickel conversion" in Figures 6 and 7. Nevertheless, optimization of the working pH is necessary to avoid two problems: wastage of chemicals such as carbonates, pH regulation chemicals (sodium hydroxide and hydrochloric acid), and high costs of the postneutralization agent. The eventual blockage of the filter is due to the nature of the fines, mostly composed of nickel hydroxide above pH = 9.8, whereas below pH = 9.8, the fines formation was found to be negligible and no filtration problems were experienced.

## Conclusions

(1) The results suggest that the fines are mostly formed by the spontaneous nucleation of a solid phase in the liquid medium generated by a high supersaturation zone, often at the reactant inlet.

(2) The Patterson et al.[2] solubility diagram can predict accurately the nickel conversion when two solid phases are taken into account: nickel hydroxide and nickel carbonate. The model is employed to determine the pH zone of the lowest soluble nickel concentration, i.e., the maximal conversion to solid nickel.

(3) The equilibrium model may not be used to predict the removal efficiency, because it does not take into account fines formation. Hence, the experimental data of nickel removal fits the Patterson et al.[2] model well when a low supersaturation, and thus minimal fines generation, is employed within the bed. At high supersaturation (pH above 9.8 or a carbonate-to-nickel ratio above 4), a significant concentration of fines is found in the outlet stream and thus the removal of the nickel is reduced. Maximal removal efficiencies of 99.6% (ratio 2) and 97.2% (ratio 4) are found at pH = 9.8 for the synthetic stream used during the experiments. At increasing pH, the nickel conversion reaches a steady level of 100%, while the removal efficiency decreases below 80% at pH = 11 for both ratios. The Patterson et al.[2] solubility model cannot thus be employed alone for nickel removal prediction.

(4) The kinetics of precipitation are fast, and the soluble species reach near equilibrium with the solid phase only after 20 cm of bed.

A later study will aim to optimize the reactor characteristics with respect to operating parameters.

## Literature Cited

(1) Mishra, S. K. Resource recovery in waste treatment increasingly used. *Min. Eng.* **1999**, April, 29−34.

(2) Patterson, J. W.; Allen, H. E.; Scala, J. J. Carbonate precipitation for heavy metals pollutants. *J. Water Pollut. Control Fed.* **1977**, *49* (12), 2397−410.

(3) Van Dijk, J. C.; Van Ammers, M.; Graveland, A.; Nuhn, P. A. N. M. State of the art of pellet softening in The Netherlands. *Water Supply* **1986**, *4*, 223−235.

(4) Tunay, O.; Tasli, R.; Orhon, D. Factors affecting the performance of hydroxide precipitation of metals. 46th Purdue Industrial Wastes Conference Proceedings, Purdue, IN, 1992.

(5) Graveland, A.; van Dijk, J. C.; de Moel, P. J.; Oomen, J. H. C. M. Developments in water softening by means of pellet reactors. *J. Am. Water Works Assoc.* **1983**, *75* (12), 619−662.

(6) Seckler, M. M. Calcium phosphate precipitation in a fluidized bed. Ph.D. Thesis, Delft University of Technology, Delft, The Netherlands, 1994.

(7) Wilms, D. Recovery of nickel by crystallisation of nickel carbonates in a fluidised bed reactor. VTT Symposium on Non-waste Technology, Espoo, Finland, 1988.

(8) Zhou, P.; Huang, J.-C.; Wei, S. Heavy metal removal from wastewater in fluidized bed reactor. *Water Res.* **1999**, *33* (8), 1918−1924.

(9) Scholler, M.; Van Dijk, J. C.; Wilms, D. Recovery of metals by crystallization in the pellet reactor. S, VD, W, *2nd Environ. Technol. Prod. Environ. Conf.* **1987**, 294−303.

(10) Stumm, M. W.; Morgan, J. J. *Aquatic Chemistry*: *an introduction emphasizing chemical equilibria in natural waters*, 2nd ed.; John Wiley and Sons: New York, 1981.

(11) McAnally, S.; Benefield, L.; Reed, R. B. Nickel removal from a synthetic nickel-plating wastewater using sulfide and carbonate for precipitation and coprecipitation. *Sep. Sci. Technol.* **1984**, *19* (2−3), 191−217.

(12) McAnally, S.; Benefield, L.; Reed, R. B. Nickel removal from wastewater using sulfide and carbonate. *Met. Finish.* **1984**, *82* (11), 29−34.

(13) Patterson, J. W. Effect of carbonate ion on precipitation treatment of cadmium, copper, lead and zinc. *36th Proceedings of the Industrial Waste Conference*, Purdue, IN, 1982.

(14) Van Rosmalen, G. M. Crystallisation and precipitation workshop, Glenburn Lodge, South Africa, 1998.

(15) Sohnel, O.; Garside, J. *Precipitation, basic principles and industrial application*; Butterworth Heinemann: Oxford, U.K., 1992; ISBN 0 7506 1107 3.

*Received for review* April 9, 2001
*Revised manuscript received* August 8, 2001
*Accepted* August 15, 2001

IE010312Q